(e,2e) simple ionization of CO_2 by fast electron impact: use of three-center parameterized continuum wave function and Dyson orbitals

2014 J. Phys. B: At. Mol. Opt. Phys. 47 225201

(http://iopscience.iop.org/0953-4075/47/22/225201)

IOP Publishing Journal of Physics B: Atomic, Molecular and Optical Physics
J. Phys. B: At. Mol. Opt. Phys. **47** (2014) 225201 (7pp) doi:10.1088/0953-4075/47/22/225201

(e,2e) simple ionization of CO_2 by fast electron impact: use of three-center parameterized continuum wave function and Dyson orbitals

O Alwan[1], O Chuluunbaatar[2,3], X Assfeld[4], A Naja[5] and B B Joulakian[1]

[1] Universitè de Lorraine, SRSMC (UMR CNRS 7565), 1 bld Arago, bat. ICPM 57078 Metz Cedex 3, France
[2] Joint Institute for Nuclear Research, Dubna, Moscow Region 141980, Russia
[3] National University of Mongolia, Ulaanbaatar, Mongolia
[4] Universitè de Lorraine, SRSMC (UMR CNRS 7565), 54506 Vandoeuvre-lès-Nancy Cedex, France
[5] Lebanese University, LPM, EDST, Tripoli, Lebanon

E-mail: boghos.joulakian@univ-lorraine.fr

Received 22 July 2014, revised 3 September 2014
Accepted for publication 12 September 2014
Published 28 October 2014

Abstract

The variation of the triple differential cross section of the (e,2e) simple ionization of CO_2 with the direction of the ejected electron is studied. The calculations are performed in the frame of a perturbative first Born procedure, using a three-center Dyson type description for the $1\pi_g$ bound electron and an approximate three-center continuum solution of the corresponding Schrödinger equation for a specific wave vector $\mathbf{k}_e$ for the free ejected electron, which satisfies the correct asymptotic boundary condition up to the order $O((kr)^{-2})$. Empirical values for the screening of the three nuclei of the target and for the Sommerfeld parameters of the three-center Coulomb continuum function are introduced. The results are compared to existing experimental results and a theoretical result obtained by the same approach, using a Hartree–Fock Slater type orbital.

Keywords: inelastic electron-molecule collision, ionization of CO2, Dyson orbitals, two center continuum

1. Introduction

The simple (e,2e) ionization by electron impact, which consists in coincidence detection of the ejected and the scattered electrons emerging from a mono-collision of an electron with an atomic or molecular gas, is an excellent tool for studying the electronic structure of the target, the nature of the interactions involved, and the mechanisms of the inelastic collision [1–3]. Compared to the ionization of atoms, the theoretical treatment of this process in the case of molecules presents supplementary difficulties. Here the orientation of the target during the inelastic collision and the vibrational and rotational states must be taken into account. Moreover, the description of the ejected electron in the field of many attractive centers needs an appropriate continuum multi-center wave function. Now, as the vibrational and rotational levels involved cannot be resolved by the actual (e,2e) setups, the closure relation is used over these levels. See [4] for a clear explanation on this point. Here the ionization is considered as a vertical transition from the electronic ground state at the equilibrium internuclear distance to the ground state of the residual ion at the same internuclear distance.

An area of concern is the multi-center aspect of the wave function of the ejected electron. Generally, one center partial wave developments are used, which require large number of terms and are not well adapted to the multi center nature of molecules. The other alternative is to use, for linear molecules, the many center development in spheroidal coordinates [5], which would be appropriate if it did not demand very large computational efforts. To avoid these inconveniences, a

two-center Coulomb continuum (TCC) wave function in a closed form, satisfying the correct boundary conditions approximately, was developed in the past [6, 7]. This TCC model was recently extended to three-center targets and applied to the ionization of CO_2 [8], for which simple (e,2e) detections were realized by the Manchester group for the low equal energy sharing regime [9] and by the Orsay group for the relatively higher incident energy asymmetric regime [10]. This multicentric model is now considered to be an appropriate choice for the description of the electron in other situations, such as the field of high harmonic generation by ultra short pulsed lasers [11–13] on diatomic systems.

The aim of the present work is to introduce improvements to the last theoretical attempt [8], which failed to reproduce the expected 'recoil lobe' around the direction of the momentum transfer in the variation of the multiple differential cross sections (MDCS) observed experimentally [10]. In this work, we try to go beyond the Hartree–Fock description of the bound electron in the initial state of the colliding system and introduce, for the first time, the Dyson $1\pi_g$ Gaussian orbital, which is obtained from coupled cluster [14, 15] results by calculating the overlap between the N state of the target and the $(N-1)$ state of the singly ionized ion [16]. The practical aspect of this choice is that Gaussian functions nowadays are more often available, especially for complex molecules, so the present work can open the way for future calculations on more complex linear systems. We adopt also, in the interaction of the incident electron with the three centers of the target, a parametric description of the screening due to the inactive electrons. We use, as in [8], the empirical charges for the wave function of the ejected electron, satisfying the asymptotic condition.

2. Theory

We employ, as in [8], a perturbative first Born procedure for the determination of the MDCS of the simple ionization of the three-center collinear molecule CO_2 in a given orientation. For the ionization of the $1\pi_g$ orbital, it can be given in atomic units by:

$$\sigma^{(4)}(\rho) = \frac{\mathrm{d}^4\sigma}{\mathrm{d}\Omega_\rho \mathrm{d}\Omega_s \mathrm{d}\Omega_e \mathrm{d}\left(k_e^2/2\right)} = \frac{k_s k_e}{2k_i}\left(\left|T_{fi}^{m=-1}\right|^2 + \left|T_{fi}^{m=1}\right|^2\right). \quad (1)$$

As shown in figure 1, ρ represents the internuclear vector of the target CO_2, with θ_ρ and ϕ_ρ the polar and azimuthal angles, respectively, defined in the fixed laboratory frame. The modulus $\rho = 4.39$ a.u. at the equilibrium position. The elements of solid angles $\mathrm{d}\Omega_s$, $\mathrm{d}\Omega_e$, and $\mathrm{d}\Omega_\rho$ are respectively, those of the orientations of the scattered and the ejected electrons and that of $\boldsymbol{\rho}$. We represent the incident, scattered, and ejected electrons by their wave vectors $\mathbf{k}_i$, $\mathbf{k}_s$, and $\mathbf{k}_e$. Finally, m is the electronic magnetic quantum number corresponding to the level from which the electron is ejected. Here $m = \pm 1$ for the $1\pi_g$ electron.

As the collision takes place at any orientation of the target, we have to integrate overall possible and equally probable directions of the molecule in space and obtain the triple differential cross section (TDCS):

$$\sigma^{(3)} = \frac{1}{4\pi}\int \mathrm{d}\Omega_\rho \sigma^{(4)}(\boldsymbol{\rho}). \quad (2)$$

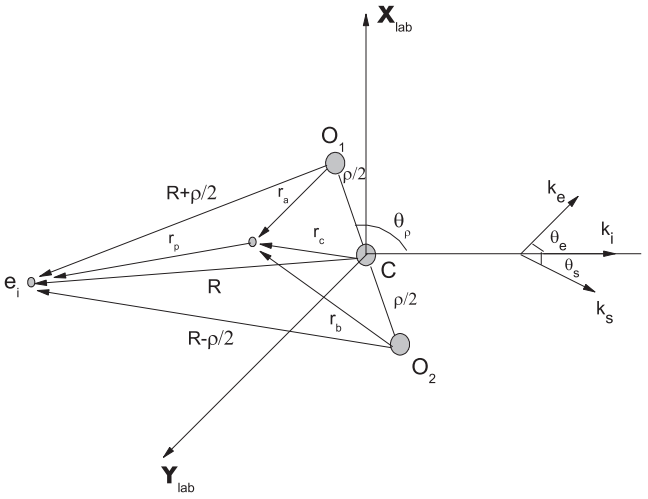

Figure 1. The reference frame with the different wave vectors $\mathbf{k}_i$, $\mathbf{k}_s$, and $\mathbf{k}_e$, representing the momenta of the incident, scattered, and ejected electrons, respectively, and the different position vectors of the incident and ejected (bound) electrons with respect to the three nuclei.

We define E_i, E_s, and E_e as the energy values of the incident, scattered, and ejected electrons, respectively. They must satisfy the following energy conservation equation

$$E_i = E_s + E_e + I, \quad (3)$$

with $I = 13.77$ eV representing the energy necessary to eject an electron from the $1\pi_g$ orbit of the CO_2 target [9, 17].

In our model we will consider only the active electron of the target. So the transition matrix element T_{fi}^m will involve only two electrons, the fast incident (scattered) and the bound (slow ejected) electrons. The positions of these two electrons in the body fixed system of reference are given by $\mathbf{R}$ and $\mathbf{r}$. The carbon atom is at the origin of this system, and the two oxygen atoms are placed on the z axis at equal distances from the carbon. Considering only the first order term of the Born series we will have:

$$T_{fi}^m = \frac{1}{2\pi}\int \mathbf{dr}\int \mathbf{dR} \times \exp\left(\imath\left(\mathbf{k}_i\mathbf{R} - \mathbf{k}_s\mathbf{R}\right)\right)\bar{\lambda}_f(\mathbf{r},\boldsymbol{\rho})\, V\, \lambda_i^m(\mathbf{r},\boldsymbol{\rho}). \quad (4)$$

Here, the plane waves describe the fast incident and scattered electrons. $\lambda_i^{m=\pm 1}(\mathbf{r},\boldsymbol{\rho})$ is the Dyson orbital [16, 18] of the bound electron in the initial state in the body fixed system of reference, and $\lambda_f(\mathbf{r},\boldsymbol{\rho})$ is the wave function of the ejected electron. The position of this electron with respect to the two oxygen centers O_1 and O_2 will then be given by $\mathbf{r}_{O_1} = \mathbf{r} + \boldsymbol{\rho}/2$ and $\mathbf{r}_{O_2} = \mathbf{r} - \boldsymbol{\rho}/2$. The perturbation V, due to the interaction of the incident electron with the target, will be approximated by the following model potential borrowed from [19], which takes into consideration the effect of the screening due to the

inactive electrons in the molecule:

$$V = U(\mathbf{R}) + \frac{1}{|\mathbf{R}-\mathbf{r}|}, \tag{5}$$

with

$$U(\mathbf{R}) = a\Big(V_{O_1}\Big(\mathbf{R}+\boldsymbol{\rho}/2\Big) + V_C(\mathbf{R}) + V_{O_2}(\mathbf{R}-\boldsymbol{\rho}/2)\Big), \tag{6}$$

and

$$V_C(\mathbf{R}) = -\frac{1}{R}\Big(z_C + N_{1C}\exp\left(-\alpha_C R\right) + N_{2C}\exp\left(-\beta_C R\right)\Big),$$

$$V_O(\mathbf{R}\pm\boldsymbol{\rho}/2) = -\frac{f_\pm\left(\theta_\rho\right)}{|\mathbf{R}\pm\boldsymbol{\rho}/2|} \times \Big(z_O + N_{1O}\exp\left(-\alpha_O\left|\mathbf{R}\pm\boldsymbol{\rho}/2\right|\right) + N_{2O}\exp\left(-\beta_O\left|\mathbf{R}\pm\boldsymbol{\rho}/2\right|\right)\Big). \tag{7}$$

Here, we have introduced the following polarization factor, which varies with the orientation of the target

$$f_+\left(\theta_\rho\right) = \left(1-\frac{\sin\left(\theta_\rho\right)}{2}\right),$$

$$f_-\left(\theta_\rho\right) = \frac{\sin\left(\theta_\rho\right)}{2} \quad 0 \leqslant \theta_\rho \leqslant \frac{\pi}{2},$$

$$f_+\left(\theta_\rho\right) = \frac{\sin\left(\theta_\rho\right)}{2},$$

$$f_-\left(\theta_\rho\right) = \left(1-\frac{\sin\left(\theta_\rho\right)}{2}\right) \quad \frac{\pi}{2} \leqslant \theta_\rho \leqslant \pi. \tag{8}$$

Using the Bethe transformation for the position vector $\mathbf{R}$ of the incident fast electron in equation (4)

$$\int \mathbf{dR}\,\frac{\exp\left(\imath\mathbf{KR}-\alpha|\mathbf{R}-\mathbf{r}|\right)}{|\mathbf{R}-\mathbf{r}|} = \frac{4\pi\exp\left(\imath\mathbf{Kr}\right)}{\alpha^2+K^2}, \tag{9}$$

with $\mathbf{K} = \mathbf{k}_i - \mathbf{k}_s$ the momentum transfer, the transition matrix element for a given value of m will be reduced to

$$T_{fi}^m = 2\int \mathbf{dr}\bar{\lambda}_f(\mathbf{r},\boldsymbol{\rho})\lambda_i^m(\mathbf{r},\boldsymbol{\rho}) \times\left(\frac{\exp\left(\imath\mathbf{Kr}\right)}{K^2} + a\left(-\frac{z_C}{K^2}-\frac{N_{1C}}{\alpha_C^2+K^2}-\frac{N_{2C}}{\beta_C^2+K^2}\right.\right. + f_+\left(\theta_\rho\right)\left(-\frac{z_{O_1}}{K^2}-\frac{N_{1O}}{\alpha_O^2+K^2}-\frac{N_{2O}}{\beta_O^2+K^2}\right)\exp\left(-\imath\mathbf{K}\boldsymbol{\rho}/2\right) + f_-\left(\theta_\rho\right)\left(-\frac{z_{O_2}}{K^2}-\frac{N_{1O}}{\alpha_O^2+K^2}-\frac{N_{2O}}{\beta_O^2+K^2}\right) \times\exp\left(\imath\mathbf{K}\boldsymbol{\rho}/2\right)\Big)\Big). \tag{10}$$

The integrations run over the space coordinates of the ejected electron.

We have done five types of calculations with different model potential parameters for the interaction of the incident electron with the target. The first type corresponds to that applied in [8], where the three centers are considered as screened Coulomb centers with Z_a representing the positive value of the nuclear charge of the oxygen center, as in the Sommerfeld parameter in equation (13) obtained by the asymptotic condition, which imposes that $z_{O_1} + z_C + z_{O_2} = 1$ at very large distances from the residual ion. Taking $z_{O_1} = z_{O_2} = Z_a$, we must have $z_C = 1 - 2Z_a$. The second type corresponds to the same calculation but with the angular polarization factor $f_\pm(\theta_\rho)$. In the third and fourth types, we assimilate the interaction to that of an electron with three protons. In the fifth type, we introduce the model potential of [19], described above.

2.1. The initial state wave function

It is useful to recall that the ground state configuration of CO_2 is given by [20, 21]

$$1\sigma_g^2 1\sigma_u^2 2\sigma_g^2 3\sigma_g^2 2\sigma_u^2 4\sigma_g^2 3\sigma_u^2 1\pi_u^4 1\pi_g^4. \tag{11}$$

The incident electron will eject a $1\pi_g$ electron, which will be described by the following Dyson orbital [16, 18] obtained from coupled cluster [14, 15] results, constructed by linear combinations of Gaussian type orbitals centered on the two oxygen centers O_1 and O_2 and the carbon center C. It is given by $\lambda_i^{m=\pm1}(\mathbf{r},\rho) = 2^{-1/2}(f_g \pm \imath g_g)$, where

$$f_g = A\left(2p_{x_1}^{O_2} - 2p_{x_1}^{O_1}\right) + B\left(2p_{x_2}^{O_2} - 2p_{x_2}^{O_1}\right) + E\left(3d_{xz}^{O_2} + 3d_{xz}^{O_1}\right) + F\,3d_{xz}^{C}$$

$$g_g = A\left(2p_{y_1}^{O_2} - 2p_{y_1}^{O_1}\right) + B\left(2p_{y_2}^{O_2} - 2p_{y_2}^{O_1}\right) + E\left(3d_{yz}^{O_2} + 3d_{yz}^{O_1}\right) + F\,3d_{yz}^{C}, \tag{12}$$

and the upper index indicates the atom on which a given orbital is centered. The orbitals are defined by

$$2p_{x_1} = x\Big(C_1\exp\left(-b_1r^2\right) + C_2\exp\left(-b_2r^2\right) + C_3\exp\left(-b_3r^2\right)\Big),$$

$$2p_{x_2} = C_4 x\exp\left(-b_4r^2\right), \quad 3d_{xz} = C_5 xz\exp\left(-b_5r^2\right),$$

$$2p_{y_1} = y\Big(C_1\exp\left(-b_1r^2\right) + C_2\exp\left(-b_2r^2\right) + C_3\exp\left(-b_3r^2\right)\Big),$$

$$2p_{y_2} = C_4 y\exp\left(-b_4r^2\right), \quad 3d_{yz} = C_5 yz\exp\left(-b_5r^2\right).$$

Here the Mulligan convention [20] is used, where all one-center orbitals have the same z axis along the internuclear axis ρ. They are all positive in the positive z direction.

The optimized orbital exponents b_1, b_2, b_3, b_4, and b_5 of oxygen and carbon are shown in table 1. The corresponding coefficients in the Gaussian function are C_i and are displayed in table 2, and the corresponding coefficients A, B, E, and F of the $1\pi_g$ level are shown in table 3.

Table 1. Optimized orbital exponents b_1, b_2, b_3, b_4, and b_5 of oxygen and carbon.

b_1	b_2	b_3	b_4	b_5
15.539 616	3.599 933 6	1.013 761 8	0.270 005 8	0.8

Table 2. The coefficients C_1, C_2, C_3, C_4, and C_5 of the molecular orbitals of CO_2.

C_1	C_2	C_3	C_4	C_5
0.070 874 3	0.339 752 8	0.727 158 6	1	1

Table 3. The coefficients A, B, E, and F for the Dyson orbital of the $1\pi_g$ level.

A	B	E	F
0.449 110 3	0.351 321 7	0.023 783 7	0.066 074 8

2.2. The final state wave function: the three-center electronic continuum

Following ionization, the relatively slow ejected electron will be found in the field of the linear CO_2^+ ion. Its wave function $\lambda_f(\mathbf{r}, \boldsymbol{\rho})$ will be given by the following three-center Coulomb continuum function proposed by [7]

$$\chi(\mathbf{k}, \mathbf{r}, \rho) = \frac{\exp(\imath\mathbf{kr})}{(2\pi)^{3/2}} \times M_a \ {}_1F_1\left(\imath\alpha_a, 1, -\imath\left[kr_a + \mathbf{kr}_a\right]\right) \times M_b \ {}_1F_1\left(\imath\alpha_b, 1, -\imath\left[kr_b + \mathbf{kr}_b\right]\right) \times M_c \ {}_1F_1\left(\imath\alpha_c, 1, -\imath\left[kr_c + \mathbf{kr}_c\right]\right), \quad (13)$$

with

$$M_j = \exp\left(-\pi\frac{\alpha_j}{2}\right)\Gamma\left(1-\imath\alpha_j\right), \quad j = a, c, b \quad (14)$$

which corresponds as indicated in [7] to an approximate solution of the Schrödinger equation, an electron having **k** as the wave vector in the Coulomb field of three fixed centers. Here ${}_1F_1$ is the Kummer confluent hypergeometric function, and $\alpha_j = -Z_j/k$ is the Sommerfeld parameter. The vectors $\mathbf{r}_a = \mathbf{r} + \boldsymbol{\rho}/2$ and $\mathbf{r}_b = \mathbf{r} - \boldsymbol{\rho}/2$ (see figure 1) refer to the positions of the ejected electron with respect to the two oxygen centers, and $\mathbf{r_c} \equiv \mathbf{r}$ that of the carbon. Following the original choice [8], we will represent the charges, in the wave function, corresponding to the two oxygen centers by $Z_a = Z_b$. Knowing that $Z_a + Z_b + Z_c = 1$ for the residual ion, we will have $Z_c = 1 - 2Z_a$. $\lambda_f(\mathbf{r}, \boldsymbol{\rho})$ is symmetrical with respect to the exchange of the vectors $\mathbf{r}_a$ and $\mathbf{r}_b$, and it satisfies the asymptotic condition:

$$\lim_{r\to\infty}\chi(\mathbf{k}, \mathbf{r}, \boldsymbol{\rho}) \to \frac{\exp(\imath\mathbf{kr})}{(2\pi)^{3/2}} \times \exp\left(-\imath(\alpha_a + \alpha_c + \alpha_b)\ln(kr + \mathbf{kr})\right). \quad (15)$$

It is clear that satisfying the asymptotic condition does not insure the quality of the three-center continuum wave function (ThCC), since the reaction region is in the first few atomic units as the initial bound state wave function leads to a fast convergence in terms of r. Nevertheless, we believe that as the ThCC is an approximate solution of the three-center Schrödinger equation [7] and by its nature posesses the three-center symmetry in contrast to other one-center continuum wave functions used for molecules, it can be considered as a good compromise.

3. Results and discussion

Our aim in this work is to go beyond what has been done in the last theoretical attempt [8] in matching the experimental results concerning the (e,2e) simple ionization of CO_2, which has succeeded, first, to show, relatively well, the right behavior of the TDCS in the region of the binary peak (see figure 1 of [8]); and, second, to give the good prediction for the optimal incident energy value around 600 eV (see figure 4 in [8]) as well as to show the expected molecular aspect of the problem in the variation of the TDCS with the scattering angle for a fixed direction of the internuclear axis. It has, on the other hand, failed to reproduce the expected and experimentally observed [10] 'recoil lobe' around the opposite direction of the momentum transfer in the variation of the TDCS. In this work, we introduce for the first time the Dyson $1\pi_g$ Gaussian orbital, which we obtained from coupled cluster [14, 15] results by calculating the overlap between the N state of the target and the $(N - 1)$ state of the singly ionized ion [16]. Our aim in this choice was to open the way for future applications of this type of orbitals, which are more available for complex molecules than the Slater type orbitals used in [8]. We adopt, for the interaction term of the incident electron with the three-center target, a parametric description of the screening due to the inactive electrons of equation (7) and introduce empirical charges Z_a, Z_b, and Z_c for the wave function of the ejected electron, satisfying the asymptotic condition as presented above.

We have performed our calculations for the same conditions as the existing experimental data, namely, the detection of the fast scattered electron, having the energy value $E_s = 500$ eV, at an angle $\theta_s = -6°$ with respect to the incidence direction, in coincidence with the ejected electron of $E_e = 37$ eV. Here the incident energy is deduced from equation (3).

To see separately the different contributions of the interaction potential terms equation (7), we present three types of results. The first is obtained by considering $V = |\mathbf{R}-\mathbf{r}|^{-1}$ in equation (5), taking only the interaction of the incident electron with the bound (ejected) electron and neglecting the nuclear terms; the second, by considering $V = U(\mathbf{R})$, where we exclude the electron–electron interaction; and the third, by taking the whole interaction of the incident electron with the molecule. For each situation we have tested, for the ejected electron continuum wave function

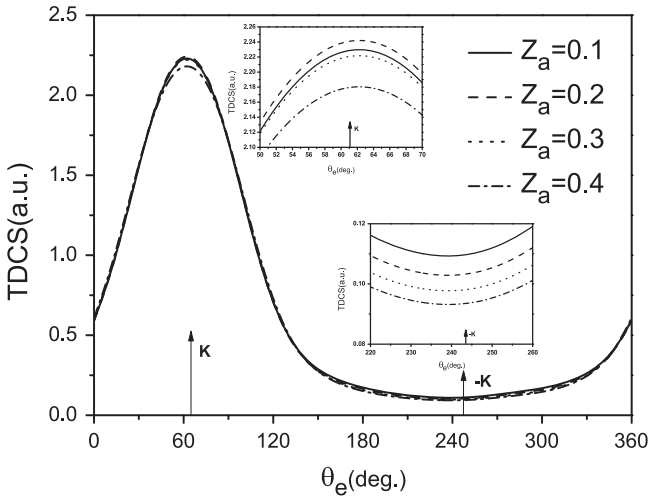

Figure 2. The variation of the TDCS for $V = |\mathbf{R} - \mathbf{r}|^{-1}$, in terms of the ejection angle θ_e of the ionization of the $1\pi_g$ level of CO_2 for four values of the empirical parameter $Z_a = 0.1$, 0.2, 0.3 and 0.4, for the final state. The energy of the scattered electron $E_s = 500$ eV, detected at an angle $\theta_s = -6°$. The energy of the ejected electron $E_e = 37$ eV.

(13), many different values are obtained for Z_a, and consequently for Z_b and Z_c , following the asymptotic condition $Z_a + Z_b + Z_c = 1$. Among these values we present only the results for $Z_a = 0.1$, 0.2, 0.3 and 0.4, which are quite representative.

Figure 2 corresponds to the first test, where $V = |\mathbf{R}-\mathbf{r}|^{-1}$. We can observe that in this choice, the variation of the charges Z_a, Z_b, Z_c in the three-center continuum wave function has a very small effect on the different curves, which present no recoil lobe. The profile of the curves does not vary. This is reasonable because in the four cases the initial state function is the same. Moreover, these charges in the continuum state are directly related to the molecular nature of the residual ion, which is ignored in the interaction potential in this try.

On figures 3(a)–(d) the results obtained for $V = U(\mathbf{R})$ are presented for $Z_a = 0.1$, 0.2, 0.3 and 0.4, respectively. Here, we take only the interaction of the incident electron with the three screened nuclei. Five different types of potentials are considered, defined in table 4. To allow comparison, all five cases are plotted on the same absolute scale in atomic units. The general observation is that the variation of Z_a, Z_b, Z_c in the TCC brings a small change in the profiles. This change is perceptible on the dotted curve (the second from below on the figures), corresponding to the type 2 potential in table 4 as it changes from a straight line for (a) $Z_a = 0.1$ to a small 'sinusoidal' structure for $Z_a = Z_b = 0.4$, $Z_c = 0.2$. In the other types, the same effect of increase in the 'amplitude' is also waypresent. This can be explained by the fact that, as we increase Z_a, the influence of the outer oxygen atoms is increased both in the ThCC function and in the potential for type 2, thus increasing the molecular aspect of the continuum wave function.

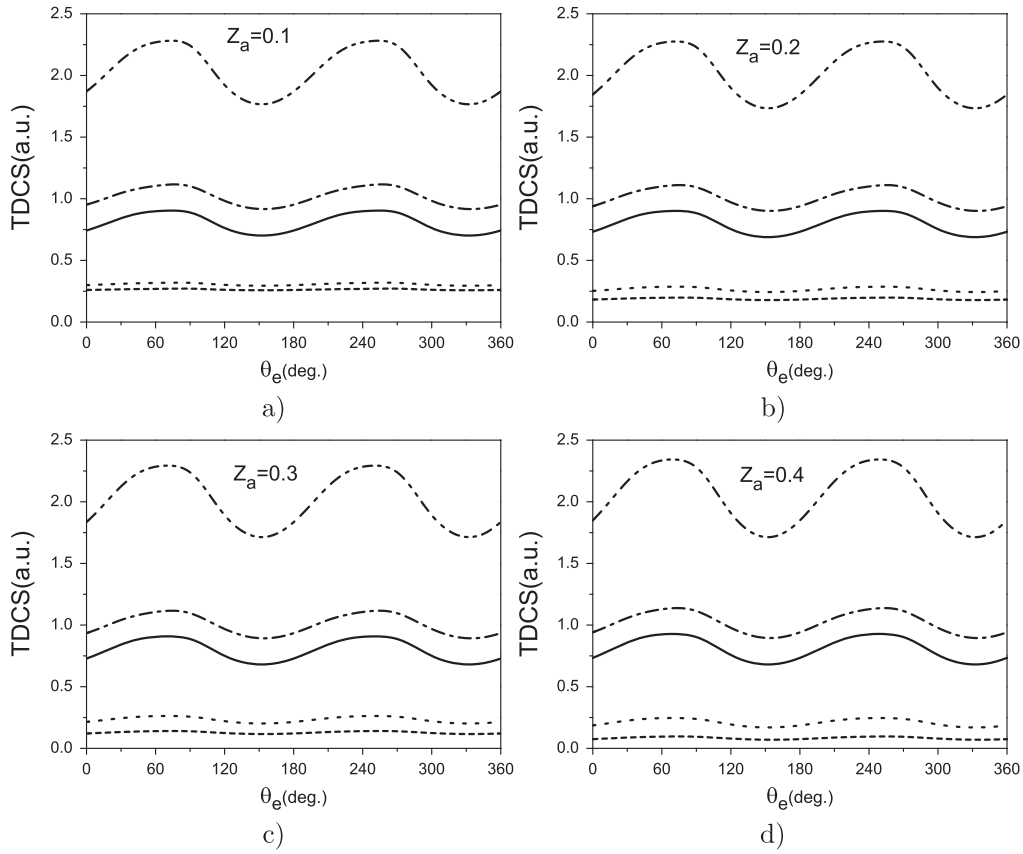

Figure 3. Same as in figure 2 but for $V = U(\mathbf{R})$. The dotted line corresponds to the results obtained by the choice type 1 of table 4. The short-dashed line to type 2, the dash-dot-dot to type 3, the dash-dot to type 4, and the full line to type 5.

Table 4. Numerical values of the coefficients and the screening parameter used in equation (7).

type	a	z_O	z_C	α_C	β_C	α_O	β_O	N_{1C}	N_{2C}	N_{1O}	N_{2O}	$f_{\pm}(\theta_\rho)$
1	1	Z_a	$1-2Z_a$	0	0	0	0	0	0	0	0	1
2	1	Z_a	$1-2Z_a$	0	0	0	0	0	0	0	0	equation (8)
3	1	1	1	0	0	0	0	0	0	0	0	1
4	1	1	1	0	0	0	0	0	0	0	0	equation (8)
5	$\frac{1}{3}$	1	1	4.714	1.110 09	6.264	1.5964	2	3	2	5	1

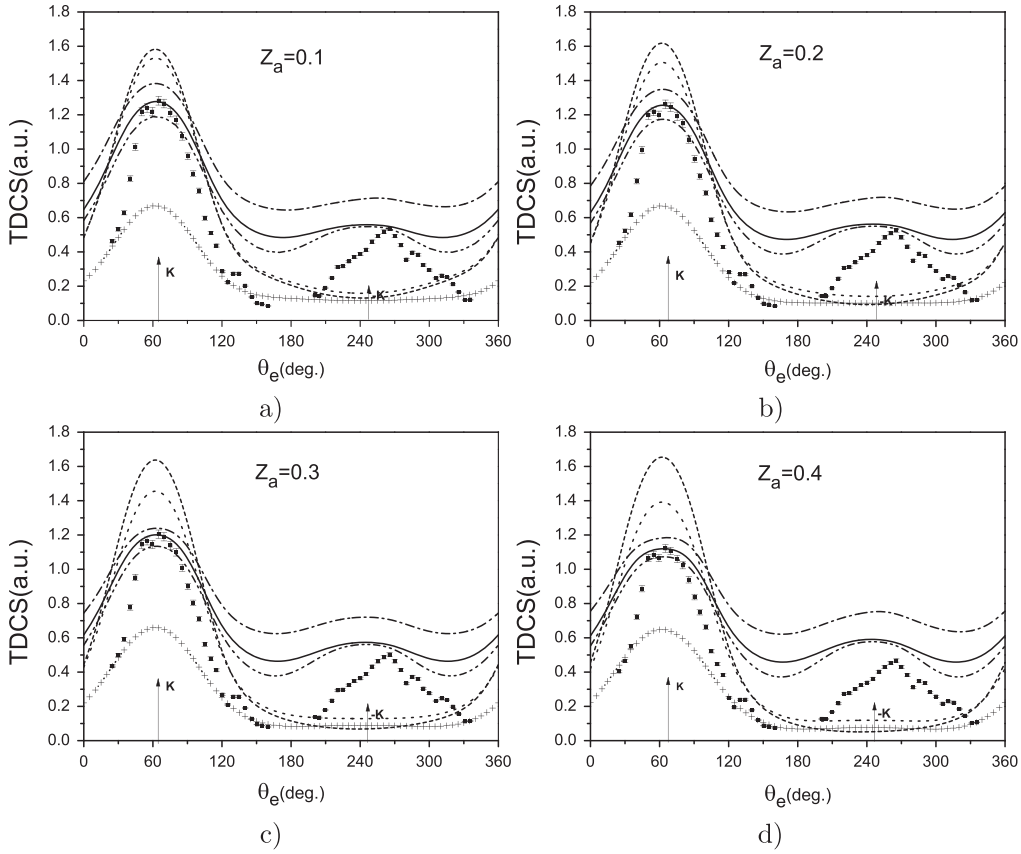

Figure 4. Same as in figure 2 but for $V = U(\mathbf{R}) + |\mathbf{R} - \mathbf{r}|^{-1}$. The curve with crosses corresponds to the past results of [8]. The experimental cross-section set [10] is normalized in such a way that the binary peak is at the same level as that of type 5.

Figure 4 corresponds to the variation of the TDCS (equation (2)) with both terms of perturbation V in the transition matrix element. All the theoretical results are given in the same scale. The experimental result is normalized in such a way as to have the maximum of the experimental point on the same level as that of the continuous curve, corresponding to the potential of type 5 in table 4. We first compare the dotted curve to the one with crosses, which represent, respectively, the results obtained by the Dyson Gaussian type orbitals and the Hartree–Fock Slater type orbitals, corresponding both to the type 1 in table 4. We observe that the introduction of the Dyson orbitals for the same perturbation, i.e., type 1 potential, produces no recoil peak and changes only the magnitude of the TDCS, keeping the structure unchanged. So we can be assured that Dyson Gaussian type orbitals, which can be more available than Slater type orbitals, especially for complex molecules, are as well adapted as the Slater type orbitals.

We then pass to the line with short dashes in figure (4), which corresponds to the type 2 potential for the interaction of the incident electron with the target, and where an angular polarization of the charges is introduced, as defined in equation (8). It does not bring any significant improvement either in the recoil region.

The dash-dot-dot and the dash-dot curves, which both correspond to the case for which a pure Coulomb interaction with unit charges is considered for the perturbation potential, produce the expected recoil peak. Here also the introduction of the angular polarization in type 4 does not modify significantly the results with respect to type 3.

A general observation of these results can be that the interaction of the incident electron with nuclei plays an important role for the ejection in the recoil region. In fact, the recoil momentum $\mathbf{q} = \mathbf{K} - \mathbf{k}_e$ of the target, which is obtained by the conservation of the total momentum, reaches its

maximum value when the momentum of the ejected electron $\mathbf{k}_e$ is anti parallel to the momentum transfer **K**. Now, in this situation, the residual ion moves in the opposite direction to the ejected electron. This happens when the interaction of the incident electron with the target, which will create this movement of the residual ion, is well described, which is apparently the case for types 3 and 4.

This semiclassical interpretation of the existence of the recoil peak does not take into consideration the second order quantum effects, which we have ignored in the first Born treatment. This can explain the observation that the experimental recoil peak is not situated exactly on the direction of **–K** but is slightly translated to the right. We will in a future work try to introduce the second order terms to try to match the experimental result.

Let us now observe the decrease of the ratio of the binary peak to that of the recoil peak with Z_a. This is perceptible for the potential of type 3 represented by the dash-dot-dot curves in figure 4. We think that this must be caused by the increase of the influence of the outer oxygen centers and the reduction of the influence of the carbon situated on the center of the system as we mentioned above, thus increasing the three-center aspect of the continuum wave function.

The variation of the TDCS with the incident energy value has shown globally the same behavior as in [8], with the optimal value around 600 eV. The molecular aspect, which manifests itself in the interference structure of the variation of MDCS for a fixed orientation of the molecule with the ejection or scattering angle, was also similar to that obtained in [8].

4. Conclusion

We have applied a three-center Coulomb continuum function, obtained by the calculation of the Schrödinger equation of a free electron (with wave vector **k**) in the Coulomb field of three fixed charged nuclei, to the (e,2e) ionization of CO_2, whose electronic structure is described by Dyson orbitals. We observe that in contrast to the binary peak, whose angular position is the same as the experimental one, the recoil peak can be obtained only when special care is employed in the choice of the parameters for the interaction of the incident electron, with the three atoms constituting the target. We see also that second order terms in the transition matrix element must be introduced to try to move the theoretical recoil peak toward the higher angles to match the experimental result.

Acknowledgements

We thank the Lebanese association 'Laser' for financial support to OA The work was supported partially by the Russian Foundation for Basic Research Grant 11-01-00523 and the JINR theme 05-6-1119-2014/2016 'Methods, Algorithms and Software for Modelling Physical Systems, Mathematical Processing and Analysis of Experimental Data'.

References

[1] McCarthy I E and Weigold E 1991 *Rep. Prog. Phys.* **54** 789–879
[2] Coplan M A, Moore J H and Doering J P 1994 *Rev. Mod. Phys.* **66** 985–1014
[3] Weigold E and McCarthy I E 1999 *Electron Momentum Spectroscopy* (New York: Kluwer/Plenum)
[4] Iijima T, Bonham R A and Ando T 1963 *J. Phys. Chem.* **67** 1472–4
[5] Serov V V, Joulakian B B, Pavlov D V, Puzynin I V and Vinitsky S I 2002 *Phys. Rev.* A **65** 062708
[6] Joulakian B, Hanssen J, Rivarola R and Motassim A 1996 *Phys. Rev.* A **54** 1473–9
[7] Chuluunbaatar O, Joulakian B B, Kh Tsookhuu and Vinitsky S I 2004 *J. Phys. B: At. Mol. Opt. Phys.* **37** 2607–16
[8] Chuluunbaatar O and Joulakian B B 2010 *J. Phys. B: At. Mol. Opt. Phys.* **43** 155201
[9] Hussey M J and Murray A J 2005 *J. Phys. B: At. Mol. Phys.* **38** 2965–77
[10] Lahmam-Bennani A, Staicu Casagrande E M and Naja A 2009 *J. Phys. B: At. Mol. Opt. Phys.* **42** 235205
[11] Yudin G L, Chelkowski S and Bandrauk A D 2006 *J. Phys. B: At. Mol. Opt. Phys.* **39** 17–24
[12] Czapliński W, Gronowski J and Popov N 2008 *J. Phys. B: At. Mol. Opt. Phys.* **41** 035101
[13] Ciappina M F, Chirila C C and Lein M 2007 *Phys. Rev.* A **75** 043405
[14] Oana C M and Krylov A I 2007 *J. Chem. Phys.* **127** 234106
[15] Oana C M and Krylov A I 2009 *J. Chem. Phys.* **131** 124114
[16] Kaplan I G, Barbiellini B and Bansil A 2003 *Phys. Rev.* B **68** 235104
[17] Allan C J, Gelius U, Allison D A, Johansson G, Siegbahn H and Siegbahn K 1972 *J. Electron. Spectrosc. Relat. Phenom.* **1** 131–51
[18] Nicholson R J F, McCarthy I E and Weyrich W 1999 *J. Phys. B: At. Mol. Opt. Phys.* **32** 3873–86
[19] Rogers F J, Wilson B G and Iglesias C A 1998 *Phys. Rev.* A **38** 5007–20
[20] Mulligan J F 1951 *J. Chem. Phys.* **19** 347–62
[21] McLean A D 1963 *J. Chem. Phys.* **38** 1347–55